

Effects of Optical Layer Impairments on 2.5 Gb/s Optical CDMA Transmission

Helena X. C. Feng

*Lawrence Livermore National Laboratory, Livermore (LLNL), CA 94550 USA /
University of California, Davis (UCD), CA 95616 USA*
feng2@llnl.gov

Antonio J. Mendez

Mendez R&D Associates, P.O. Box 2756, El Segundo, CA 90245 USA

Jonathan P. Heritage

University of California, Davis, CA 95616 USA

William J. Lennon

Lawrence Livermore National Laboratory, Livermore, CA 94550 USA

Abstract: We conducted a computer simulation study to assess the effects of optical layer impairments on optical CDMA (O-CDMA) transmission of 8 asynchronous users at 2.5 Gb/s each user over a 214-km link. It was found that with group velocity dispersion compensation, two other residual effects, namely, the nonzero chromatic dispersion slope of the single mode fiber (which causes skew) and the non-uniform EDFA gain (which causes interference power level to exceed signal power level of some codes) degrade the signal to multi-access interference (MAI) ratio. In contrast, four wave mixing and modulation due to the Kerr and Raman contributions to the fiber nonlinear refractive index are less important. Current wavelength-division multiplexing (WDM) technologies, including dispersion management, EDFA gain flattening, and 3rd order dispersion compensation, are sufficient to overcome the impairments to the O-CDMA transmission system that we considered.

©2000 Optical Society of America

OCIS codes: (060.0060) Fiber optics and optical communications

References and links

1. D. Sarwate and M. Pursley, "Crosscorrelation properties of pseudorandom and related sequences," Proc. IEEE, **68**, 593-620 (1980).
2. K. Iversen and D. Hampicke, "Comparison and classification of all-optical CDMA systems for future telecommunication networks," Photonics East'95, Proc. SPIE **2614**, 110-121 (1995).
3. Paul E. Green, Jr., *Fiber Optic Networks*; (Prentice Hall, Englewood Cliffs, NJ; 1993); Chapter 13.
4. J. Y. Wei, "The role of DCN in optical WDM networks," OFC Technical Digest Series, FI-1 (Invited) (2000)
5. T. Pfeiffer, B. Deppisch, M. Witte, and R. Heidemann, "Optical CDMA Transmission for Robust Realization of Complex and Flexible Multiple Access Systems," OFC Technical Digest Series, WM51, (1999)
6. T. Pfeiffer, B. Deppisch, M. Witte, and R. Heidemann, "Operational Stability of a Spectrally Encoded Optical CDMA System Using Inexpensive Transmitters Without Spectral Control," IEEE Photon. Technol. Ltr., **11**, 916-918 (1999).
7. A.J. Mendez, R. M. Gagliardi, H.X.C. Feng, J.P. Heritage, and J-M. Morookian, "Strategies for Realizing Optical CDMA for Dense, High Speed, Long Span, Optical Network Applications," unpublished.
8. Khansefid, H. Taylor, and R. Gagliardi, "Design of (0,1) Sequence Sets For Pulsed Coded Systems," University of Southern California Report CSI-88-03-03, March 3, 1988.
9. M. Zirngibl, "Multifrequency Lasers and Applications in WDM Networks," IEEE Communications Interactive Magazine, 2nd Article, December (1998).
10. C. R. Doerr, "Waveguide-grating-router lasers for WDM," OFC Technical Digest Series, ThB3. (1999)
11. R. Ramaswamy and K. N. Sivarajan, *Optical Networks* (Morgan Kaufman, San Francisco, CA; 1998); Chapter 4.

12. 35 and 50 ps RZ electrical-to-optical modulated signals up to 10 Gb/s are feasible and commercially available. JDS Uniphase. Private communication; March 2000.
13. H. X. C. Feng, L. R. Thombly, W. J. Lennon, J. P. Heritage, "Computer Modeling of the National Transparent Optical Network (NTON)," Proc. LEOS 12th Annual Mtg, WP1 (Invited, 1999)
14. R. H. Stolen and Tomlinson, W.J. "Effect of the Raman part of the nonlinear refractive index on propagation of ultrashort optical pulses in fibers". J. Opt. Soc. B **9**, 565-73 (1992)
15. Sun, Y.; Srivastava, A.K.; Zhou, J.; Sulhoff, J.W. "Optical fiber amplifiers for WDM optical networks". Bell Labs Technical Journal, vol.4, (no.1), Lucent Technologies, **Jan.-Mar.** 187-206 (1999)
16. C. R. Doerr, M. Cappuzzo, E. Laswowski, A. Paunescu, L. Gomez, L. W. Stulz, and J. Gates, "Dynamic Wavelength Equalizer in Silica Using the Single-Filtered-Arm Interferometer," IEEE Photon. Technol. Ltr., **11**, 581-583 (1999).
17. Stern, M.; Heritage, J.P.; Chase, E.W. "Grating compensation of third-order fiber dispersion," IEEE J. Quan. Electr., **28**, 2742-8 (1992)

1. Introduction

Code Division Multiple Access (CDMA, for RF or optical) has the property of associating a signature with each set of transmitters and receivers; the signature is the code. The codes are derived from combinatorics and number theory. In general, the classes of codes are defined by the autocorrelation and crosscorrelation properties of the codes [1]. CDMA codes derive their multi-access features by virtue of mapping a signature into each bit of a message stream. The decoder/receiver generates an autocorrelation function if the sender and receiver are matched and a crosscorrelation function if they are not. If multiple, concurrent signals are transmitted, then the decoder/receiver detects both the autocorrelation and the crosscorrelation(s). The latter are the source of multi-access interference (MAI).

Optical CDMA (or O-CDMA) has been considered for future telecommunication applications since the mid 1990's [2]. Optical CDMA supports multiple asynchronous, concurrent users who occupy the same time slots and frequency domain. Optical CDMA is a true "tell and go" protocol [3], suitable for "just-in-time" transmission strategies which are emerging in the development of modern optical networks [4]. Successful field trials of O-CDMA, with eight users at a rate of 155 Mb/s each, over an installed 40 km fiber base with a tree topology were reported in 1999 [5,6]. The stage has been set for exploring O-CDMA for dense (> eight users), high speed (> 155 Mb/s), and long distance (> 40 km) optical networks.

Among various O-CDMA implementations, the WDM based pseudo-orthogonal "Flattened Matrix" codes are considered to be suitable for transmissions involving high density, high data rates, and long transmission spans. The design of the "Flattened Matrix" codes and the MAI suppression strategy has been described in a separate communication [7].

In addition to the MAI produced by the presence of concurrent users, transmission impairments from the optical medium can further complicate the issue of MAI suppression. Transmission impairments include, but are not limited to, group velocity dispersion (GVD), nonzero slope of GVD, fiber nonlinearities, and non-uniform gain at the erbium-doped fiber amplifiers (EDFAs, which are required for long span links). The influences of Kerr and Raman fiber nonlinearities include four-wave mixing (FWM), self-phase modulation (SPM), and cross-phase modulation (XPM). These impairments are concerns with regular WDM transmission systems as well, but they manifest themselves in somewhat different ways in O-CDMA, as we will describe in this paper.

In this paper we present a computer simulation study to assess the above-mentioned impairments in an asynchronous "Flattened Matrix" coded O-CDMA system for eight users, 2.5 Gb/s bit rate per user, and a 214-km transmission span. We then propose a strategy to overcome these impairments.

2. System description and simulation method

2.1 Implementation of O-CDMA

Pseudo-orthogonal (0,1) pulse sequences are considered appropriate for asynchronous, unipolar optical CDMA codes because they have the shortest code length for a given code

weight and code set size, while their crosscorrelation never exceeds one ('1') for any code shift [8]. The "Flattened Matrix" technique that Mendez R&D Associates developed distributes the pulse sequences into two dimensions (time and wavelength, for example). This technique takes advantage of the benefits of pseudo-orthogonal (PSO) pulse sequences while reducing their bandwidth expansion (and, incidentally, increasing the size of the code set).

Figure 1 illustrates the implementation of the flattened matrix codes where the initial PSO pulse sequence is the Golomb ruler $g(1,4)$ as defined in reference [8]. The light source is an eight-wavelength WDM multifrequency laser (MFL) [9,10]. The MFL produces wavelengths which are located on the International Telecommunication Union (ITU) grid, centered at 1555 nm, each with an output power of approximately 0 dBm. The electrical-to-optical conversion is carried out by return-to-zero (RZ) or short pulse [11] modulation of the MFL. For data rates above 1 Gb/s, an external modulator is required [12]. The RZ modulation process produces the short symbols required by the encoder. In our implementation, these short symbols, or chips, have a duration T_c given by the bit time T_b divided by twice the code length (the direct sequence part of the matrix code); i.e., we have introduced a guard time equal to $T_b/2$ which is not standard in O-CDMA. This condition on the chip time T_c assures that the crosscorrelations do not lead to excessive inter-symbol interference (ISI). This can be seen as follows: the crosscorrelation has a duration $(2L-1)*T_c$, where L is the code length, or the number of columns in the case of flattened matrix codes, and T_c is the chip time. We require that $(2L-1)*T_c < T_b$ in order to minimize the spillover of the crosscorrelation into adjacent bits, to minimize the ISI. This leads to $T_c < T_b/(2L-1) = T_b/7$, in the case of $L = 4$. This produces the guard time $T_g = T_b - L*T_c$. (To simplify the encoder/decoder implementation, we selected $T_c = T_b/8$.) The guard time also reduces the mean of the multi-access interference.

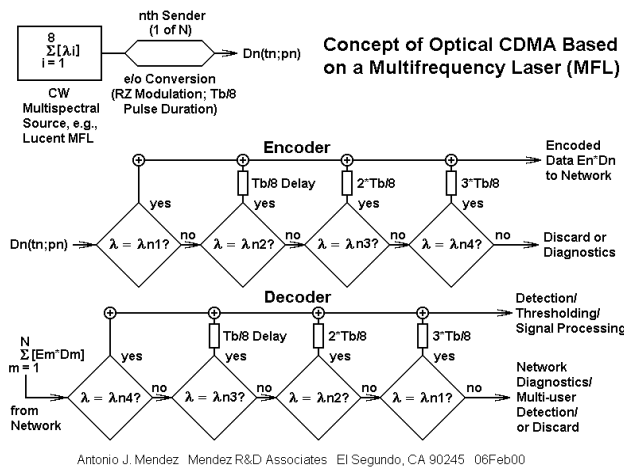


Fig 1. Implementation of the flattened matrix codes using RZ modulation electrical- to- optical conversion and encoders/decoders based on a cascade of filters and tapped delay lines.

The encoder is shown as an algorithm consisting of a cascade of wavelength filters (the code spectral sequence) and tapped delay lines to order the wavelengths. Thus, the output of the encoder is a short direct sequence of wavelength pulses. Each encoder uses four wavelengths; complementary wavelengths are discarded or used for traffic diagnostics. The decoder is the inverse sequence of wavelength filters and tapped delay lines. Uncorrelated wavelengths are used to monitor traffic, set thresholds, or multi-user detection.

2.2 The Computer simulation

An evaluation of the flattened matrix code propagation over a real link, using realistic conditions, was carried out by means of the fiber optic link simulator developed by LLNL and UCD [13]. The particular link simulated is well defined: it is a 214 km link of the National

Transparent Optical Network (NTON), running from LLNL to Sprint Advanced Technology Laboratory in Burlingame, CA. The link consists of 161.5 km of SMF-28 fiber and 52.5 km of Corning LEAF, with four EDFAs placed at strategic locations. The EDFA model used in this simulation was validated by experimental measurements of the actual devices used in NTON. The fiber model, based on a modified split-step Fourier method, was validated against an analytical soliton solution and was able to reproduce published results on Raman scattering [14]. The following optical link impairments are included in the simulation:

- power attenuation due to scattering and absorption;
- group velocity dispersion (GVD);
- 3rd order dispersion (dispersion slope);
- nonlinear refractive index;
- Raman scattering;
- gain dispersion and gain saturation in the EDFA;
- amplified spontaneous emission (ASE) produced at the EDFAs.

Presently, polarization mode dispersion (PMD) is not included at a fundamental level. However, its influence can be estimated from data published by fiber manufacturers. For the distances and bit rates employed in this study the influence of PMD is expected to be negligible (it is more important with shorter pulses and greater distances).

The test data was the nibble “1101”, encoded as a flattened matrix code and “transmitted” over the link; see Figure 2. The evaluation criteria were (1) the high fidelity transmission of the nibble, including timing of the bits and relative spacing and amplitudes of the code spectrum (ahead of the decoder) and (2) the recovery of the correlated signal by the decoder.

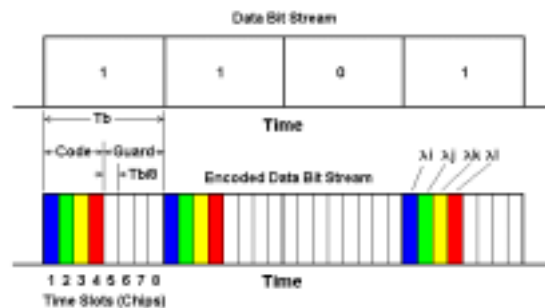


Fig 2. Illustration of test data stream “1101” used in the link propagation studies.

3. Results and discussion

3.1 Single user transmission, effect of GVD

First we study the case of a single user. Figure 3a shows the simulated encoded bit stream. The uneven power among the chips is due to the slightly non-uniform spectral output of the MFL. Figure 3b is the decoded bit stream in the back-to-back case. The decoded nibble is extremely clean because the flattened matrix code autocorrelation function has no side lobes.

Figure 4a shows the output waveform (after propagating 214 km) without GVD compensation. The bit stream was washed out completely due to the broadening of individual optical pulses (chips) caused by the GVD. The fact that the pulse width of an individual chip corresponds to that of 20 Gb/s in regular WDM transmission makes dispersion compensation absolutely necessary in this O-CDMA implementation.

We simulated the insertion of two dispersion compensating fiber modules in the link to fully compensate for the GVD at 1555 nm, the mid-point of the MFL wavelengths; the encoded nibble is then clearly visible at the output, with residual distortions and evidence of interference effects (see figure 4b). The decoded nibble is quite clean at this stage (see figure 4c). However, we expect the residual effects to become more degrading and severe in the presence of MAI, which we study next.

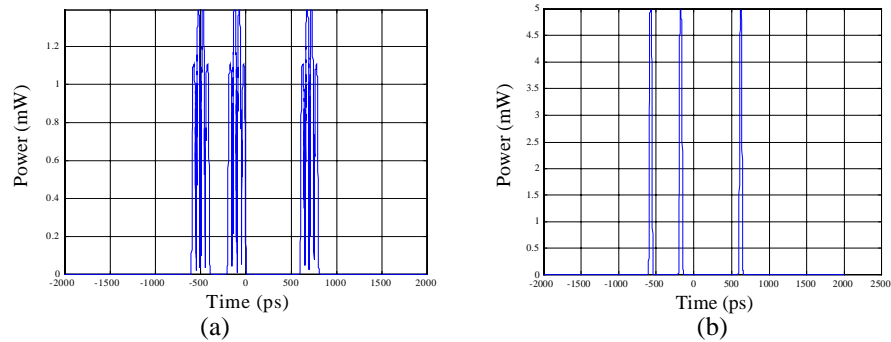


Fig 3. (a) Encoded 1101 bit stream. (b) Back-to-back decoded bit stream.

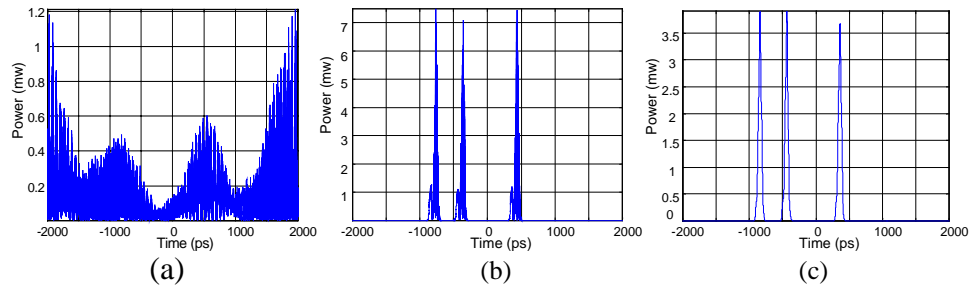


Fig 4. (a) Output “nibble” without dispersion compensation. (b) Output nibble with full group velocity dispersion (GVD) compensation at 1555 nm, prior to decoding. (c) Decoded single user nibble under (GVD) compensation.

3.2 Multi-access transmission, residual effects from full GVD compensation at 1555 nm

The residual effects that we considered include non-uniform EDFA gain, nonzero dispersion slope of the fiber, and fiber nonlinearities – nonlinear refractive index and Raman scattering. We performed a worst case study of the transmission of the 1101 bit stream of one user with all seven other users present asynchronously, assuming full GVD compensation at 1555 nm.

Figure 5a shows the superposition of eight asynchronous encoded nibbles at the input. The asynchronicity is simulated by incrementally shifting the time location of a user in the retarded time by one interval (chip time) from that of the previous user, for all users. Figure 5b is the decoded signal of a typical user (Mn3) in the back-to-back case. The autocorrelation peaks are distinctly recognizable in spite of the MAI. However, at the link output, the autocorrelation peaks are masked by the MAI, due to the residual effects (figure 5c).

Our strategy for understanding the interaction of these residual effects is to vary the simulation parameters and “turn” each effect “on”, one at a time. In this manner we examine the non-uniform gain of the EDFAs, the effects of nonzero GVD slope, and nonlinearities.

3.3 Effect of non-uniform EDFA gain

The EDFA model simulates a device in the actual NTON link. It has a typical non-uniform gain profile with saturation. No gain flattening was applied. We set the nonlinear terms and 3rd order dispersion term of the fiber to zero, with full GVD compensation at 1555 nm. Figure 6 shows the distortion of the MFL spectral profile by a cascade of four EDFAs distributed over the link. It suggests that the modified wavelength profile may cause the autocorrelation peaks of codes that are composed of low power wavelengths to be masked by the crosscorrelation functions from codes composed of wavelengths with higher power; e.g., Figure 7 shows the Mn3 autocorrelation peaks being masked by the MAI due to this effect. This finding suggests

that EDFA gain equalization [15,16] is necessary in the transmission of O-CDMA signals if the codes have a spectral content, such as flattened matrix codes have.

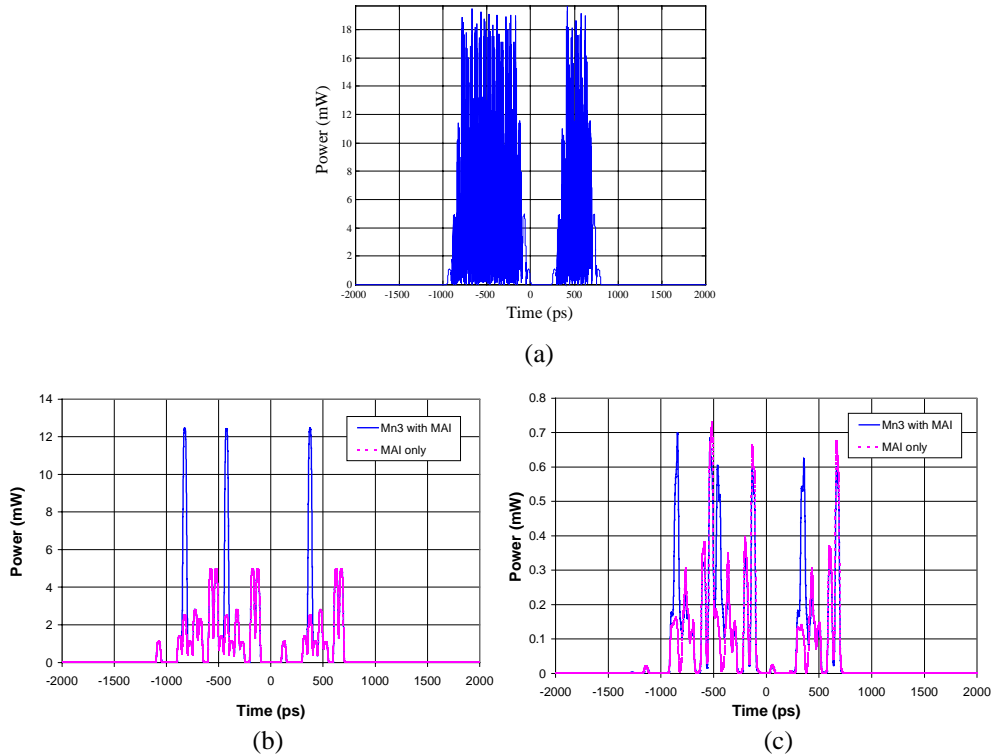


Fig 5. (a) Superposition of eight asynchronous users at input to the link. (b) Back-to-back decoder output of code Mn3 and MAI, and MAI alone. (c) Decoder output at the link output, with full GVD compensation at 1555 nm: code Mn3 masked by MAI due to residual effects.

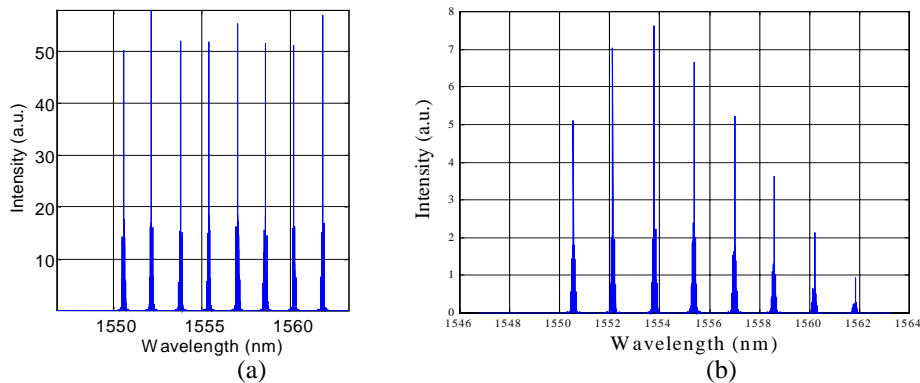


Fig 6. (a) Input wavelength profile. (b) Output wavelength profile.

3.4 Effect of nonzero slope of GVD

To study the effect of nonzero GVD slope, we used an artificially uniform gain amplifier model instead of the real EDFA model, set the nonlinear term of the fiber to zero, and used full GVD compensation at 1555 nm. The nonzero GVD slope causes different wavelengths to propagate at slightly different speed, even with full GVD compensation at the mid-point

wavelength. The variation in propagation speed causes a misalignment in the chips of a code (i.e., skew) and reduces the autocorrelation and signal to MAI ratio (figure 8). Thus, compensating for 3rd order dispersion [17] is critical at high data rates and/or over long spans.

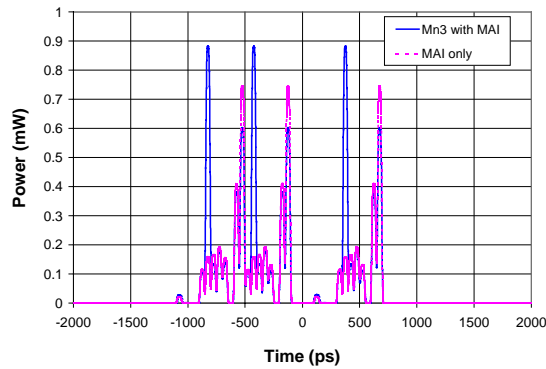


Fig 7. The MAI may mask the signal autocorrelation peaks due to non-uniform EDFA gain.

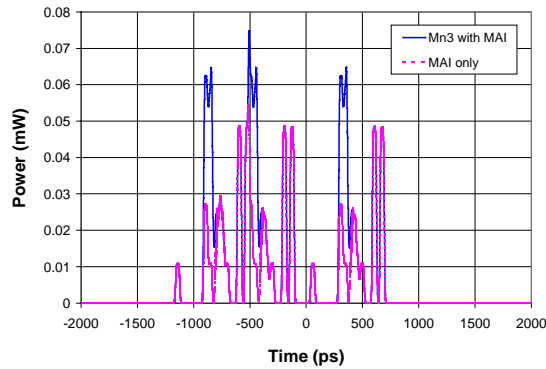


Fig 8. Effect of non-zero dispersion slope on auto- and cross- correlation output under full GVD compensation at 1555 nm, flat EDFA gain and no nonlinear effects.

3.5 Effect of nonlinearities

To study the effect of fiber nonlinearities, we used an artificially uniform gain amplifier model instead of the real EDFA model, and set the 3rd order dispersion term of the fiber to zero with full GVD compensation at 1555 nm. Both the nonlinear refractive index and the Raman terms are turned “on”. The simulation results (figure 9) show that the effect of the nonlinear terms is visible in the calculations but has negligible impact on the decoded output signal (the average transmission power is low with 8 dBm provisioned power for each EDFA, and 214 km is too short for the nonlinear effects to accumulate).

Even though the effect of nonlinearity on the overall MAI is minimal, we do observe four-wave mixing (FWM) in our simulation. Figure 10 shows the input and output spectrum of a single user, using a dB scale. FWM products are present at the output at a less than -25 dB level, but the overall change of autocorrelation peak with the MAI due to nonlinear term is not significant compared to the back-to-back case. Also, most of the FWM products are outside the wavelength bands of the decoder, thus they are discarded prior to detection.

7. Conclusion

We studied the transmission impairments of an 8 user, 2.5 Gb/s, 214 km, asynchronous optical CDMA system based on flattened matrix codes. GVD was found to be the dominant

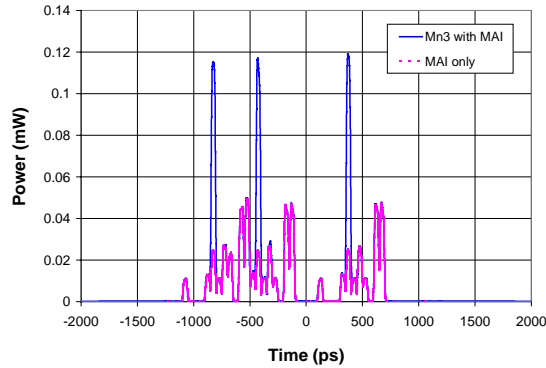


Fig 9. The nonlinear terms (nonlinear refractive index, Raman scattering) show negligible effect under full GVD compensation at 1555 nm, zero dispersion slope, and flat EDFA gain.

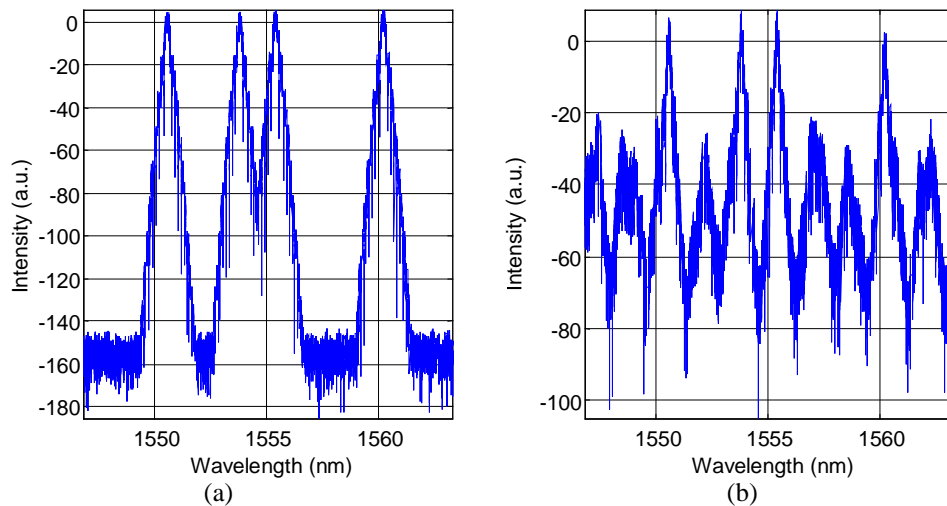


Fig 10. Four-wave mixing in the case of a single code O-CDMA transmission. (a) Input spectrum; (b) Output spectrum; both y-axes are in dB scale.

impairment; it is adequately addressed by fully compensating at the mid-point wavelength. Given full GVD compensation, the non-uniform gain profile of the EDFAs (allocating more power to the MAI than to the signal) and the 3rd order fiber dispersion (causing skew in the direct sequence part of the code) adversely affect the signal to MAI ratio. Therefore, GVD compensation at the midpoint wavelength, EDFA gain equalization, and 3rd order dispersion compensation are essential techniques in O-CDMA transmission, but nonlinearities such as the Kerr and Raman terms have a minimal effect on these O-CDMA codes. Future studies will extend this work to (a) the effect of FWM on the signal waveform and on the bit error rate; (b) systems with a higher number of users; and (c) systems with higher per-user data rates.

Acknowledgements

This effort was sponsored in part by the Department of Defense Advanced Research Projects Agency (DARPA) and the National Transparent Optical Network Consortium (NTONC), including work under the auspices of the U. S. Department of Energy under contract No. W-7405-Eng-48 at LLNL. MRDA thanks Lucent Technologies/Bell Labs for the generous grant of their MFL lasers (incorporated in the design of the O-CDMA flattened matrix codes). MRDA's effort is partially funded by the Ballistic Missile Defense Organization contract DASG60-96-C-0036, managed by the U.S. Army Space and Missile Defense Command.